Acta Crystallographica Section F
Structural Biology and Crystallization Communications
ISSN 1744-3091

Crystallization and preliminary X-ray diffraction analysis of the SOD-TAT fusion protein

Jianru Pan,[a,b] Kangjing Zhou,[b] Guangjin Zheng,[a,b] Shutao Liu[a,b]* and Pingfan Rao[a,b]*

[a]College of Bioscience and Biotechnology, Fuzhou University, 2 Xue Yuan Road, Fuzhou, Fujian 350108, People's Republic of China, and [b]Institute of Biotechnology, Fuzhou University, 523 Gongye Road, Fuzhou, Fujian 350002, People's Republic of China

Correspondence e-mail: pfrao@gmail.com, sliu@fzu.edu.cn

Received 27 February 2012
Accepted 20 March 2012

The superoxide dismutase (SOD) family of proteins are necessary to protect oxygen-utilizing cells from the toxicity of reactive oxygen species. The delivery of SOD into tissues is severely limited by its size and biochemical properties. A cell-membrane-permeable SOD, SOD-TAT, has been demonstrated to have the ability to be directly transduced into mammalian cells. In this study, the SOD-TAT fusion protein was expressed, purified and crystallized. Crystals of the SOD-TAT fusion protein diffracted to 3.20 Å resolution and belonged to space group *C*121.

1. Introduction

Superoxide dismutases (SODs) are a class of enzymes that catalyze the dismutation of superoxide into oxygen and hydrogen peroxide (Quinlan *et al.*, 1994; Tsan, 1997). There are three known forms of SOD in mammalian cells: manganese-containing superoxide dismutase (Mn-SOD), copper- and zinc-containing superoxide dismutase (CuZn-SOD) and extracellular superoxide dismutase (EC-SOD). The SOD family of proteins are necessary to protect oxygen-utilizing cells from the toxicity of reactive oxygen species (ROS).

A cell-membrane-permeable SOD was constructed by a recombinant gene technique and named SOD-TAT. The recombinant protein was a fusion of human CuZn-SOD with a cell-penetrating peptide (YGRKKRRQRRR) derived from the HIV-1 Tat protein transduction domain TAT at the C-terminus. Protein transduction domains are small peptides that are able to carry larger molecules such as peptides, full-length proteins and even 200 nm liposomes across cellular membranes (Josephson *et al.*, 1999; Lewin *et al.*, 2000; Wadia & Dowdy, 2002). They have proven to be useful in delivering biologically active cargoes both in cell culture and *in vivo* in animal models. It has been demonstrated that SOD-TAT can be directly transduced into mammalian cells across the lipid membrane barrier (Kwon *et al.*, 2000). Subsequent research has shown that SOD-TAT is effective in protecting against ischaemic brain injury, preventing and treating damage to guinea pig skin caused by single-dose UVB radiation *etc.* (Kim *et al.*, 2005; Pan *et al.*, 2009, 2010).

To understand the biochemical function of SOD-TAT, it would be valuable to determine its three-dimensional crystal structure. In this study, we report the expression in *Pichia pastoris*, purification and crystallization of the SOD-TAT fusion protein. In addition, diffraction data were collected from SOD-TAT crystals and processed to 3.20 Å resolution. These results will provide the basis for the ultimate structure determination of SOD-TAT, which should shed light on the biochemical role of this protein in the cell-penetration process.

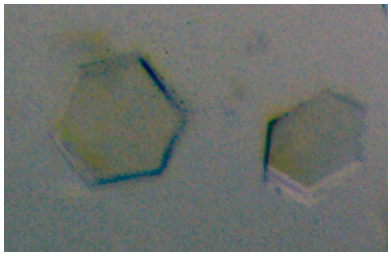

2. Materials and methods

2.1. Construction of SOD-TAT expression strain

According to a previously described procedure (Liu *et al.*, 2003), *Xho*I and *Xba*I sites were introduced into the 5′ and 3′ ends of the coding region of SOD-TAT in pBluescript II SK(+) (pBS) plasmid synthesized by Shango Bioengineering Co. Ltd (Shanghai, People's Republic of China). The SOD-TAT product was digested with *Xho*I and *Xba*I and subcloned into pPICZαA (Invitrogen, USA) digested with *Xho*I and *Xba*I, generating the recombinant plasmid

pPICZαA-SOD-TAT, which contains the cDNA of SOD-TAT downstream of an α-factor signal sequence between AOX promoter and terminator. 10 µg pPICZαA-SOD-TAT was linearized by *Sac*I and integrated into the genome of *P. pastoris* strain X-33 by electroporation. Transformants were plated on YPDS plates containing 100 µg ml^{-1} Zeocin. Zeocin-resistant colonies were used as expression strains.

2.2. Expression of SOD-TAT

A Zeocin-positive colony was inoculated into 100 ml YPD medium containing 100 µg ml^{-1} Zeocin and incubated at 303 K for 1 d with shaking at 200 rev min^{-1}. The cells were harvested, washed with sterilized water and resuspended in BSM medium. Recombinant SOD-TAT was expressed for 8 d at 303 K according to the *Pichia* Fermentation Process Guidelines (Invitrogen); 1.0% methanol was added every 24 h to induce secretion of SOD-TAT.

2.3. Protein purification

2 g lyophilized protein powder was dissolved in 10 ml 20 m*M* phosphate–citrate buffer solution pH 6.0 and centrifuged (10 000*g*, 10 min). The clear supernatant was desalted and applied onto a UNOsphere S ion-exchange chromatography column (Bio-Rad; 1.6 × 10 cm) pre-equilibrated with 20 m*M* phosphate–citrate buffer pH 6.0 at room temperature at a flow rate of 1 ml min^{-1}. Elution was carried out with a step gradient of 20 m*M* phosphate–citrate buffer containing 0.4 and 1 *M* NaCl. The purity of the protein was verified by SDS–PAGE and Coomassie Blue staining. The peak fraction with SOD activity was pooled, desalted, concentrated to 36 mg ml^{-1} and stored at 253 K until use.

2.4. Crystallization and X-ray data collection

Initial conditions for crystallization were screened using an in-house PEG screening kit. Crystallization trials for SOD-TAT fusion protein were performed at 287 K using the hanging-drop vapour-diffusion method in 24-well plates. Typically, 2 µl reservoir solution was mixed with 2 µl protein solution and equilibrated against 1 ml reservoir solution. A complete diffraction data set was collected on beamline BL17U1 at Shanghai Synchrotron Radiation Facility (SSRF; People's Republic of China). Diffraction experiments were conducted at 100 K and the images were recorded with an ADSC Q315r CCD area detector. The data set was collected at a wavelength of 0.9792 Å and was processed to 3.20 Å resolution. Intensity data were integrated and scaled using the *HKL*-2000 suite (Otwinowski & Minor, 1997).

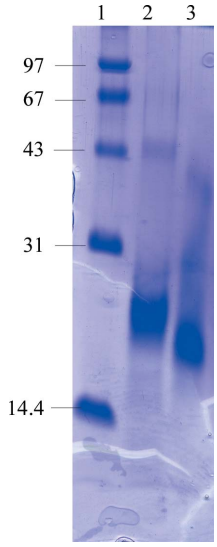

Figure 1
Purification of SOD-TAT fusion protein. Protein samples were analyzed using 12.5% SDS–PAGE followed by Coomassie Blue staining. Lane *M*, protein molecular-weight marker (labelled in kDa); lane 1, reduced SOD-TAT; lane 2, nonreduced SOD-TAT.

Table 1
Data-collection statistics.

Values in parentheses are for the highest resolution shell.

Beamline	BL17U1, SSRF
Wavelength (Å)	0.9792
Crystal-to-detector distance (mm)	400
Oscillation range per frame (°)	1
Resolution (Å)	50.0–3.20 (3.26–3.20)
Space group	*C*121
Unit-cell parameters (Å, °)	a = 181.83, b = 112.58, c = 82.57, β = 111.74
No. of molecules per asymmetric unit	6
Matthews coefficient (Å^3 Da^{-1})	3.85
Solvent content (%)	68.03
No. of observed reflections	498872
No. of unique reflections	24396
Completeness (%)	95.5 (96.9)
Multiplicity	20.4
Average $I/\sigma(I)$	14.1 (3.0)
$R_{\rm merge}$† (%)	11.5 (39.3)

† $R_{\rm merge} = \sum_{hkl}\sum_i |I_i(hkl) - \langle I(hkl)\rangle| / \sum_{hkl}\sum_i I_i(hkl)$, where $I_i(hkl)$ is the intensity of observation i of reflection hkl and $\langle I(hkl)\rangle$ is the mean intensity of reflection hkl.

3. Results

SOD-TAT fusion protein was overproduced in *P. pastoris* and purified to homogeneity by UNOsphere S ion-exchange chromatography (Fig. 1). The protein was concentrated to 36 mg ml^{-1} for crystallization trials.

After one week, small crystals of SOD-TAT were obtained from 0.1 *M* sodium chloride, 0.05 *M* Tris–HCl pH 8.0, 12%(*w*/*v*) PEG 3350. Many variables were changed in order to obtain diffraction-quality crystals, including the type of salt, the pH of the Tris–HCl buffer, the concentration of PEG 3350 *etc*. After further optimization, diffracting crystals (Fig. 2) were obtained using 0.05 *M* magnesium chloride, 0.05 *M* Tris–HCl pH 8.5, 15%(*w*/*v*) PEG 3350, 2.5%(*v*/*v*) glycerol.

Crystals of the SOD-TAT fusion protein diffracted to 3.20 Å resolution and belonged to the monoclinic space group *C*121, with

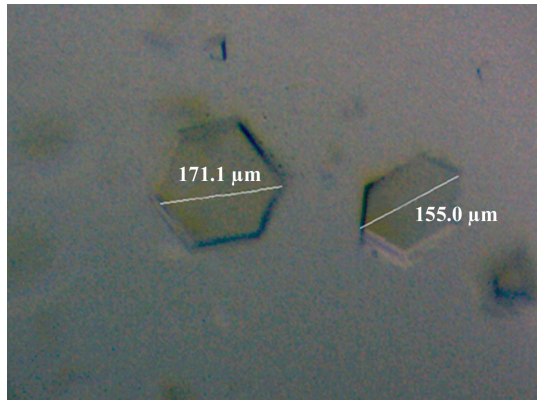

Figure 2
Crystals of SOD-TAT fusion protein grown using the hanging-drop vapour-diffusion method.

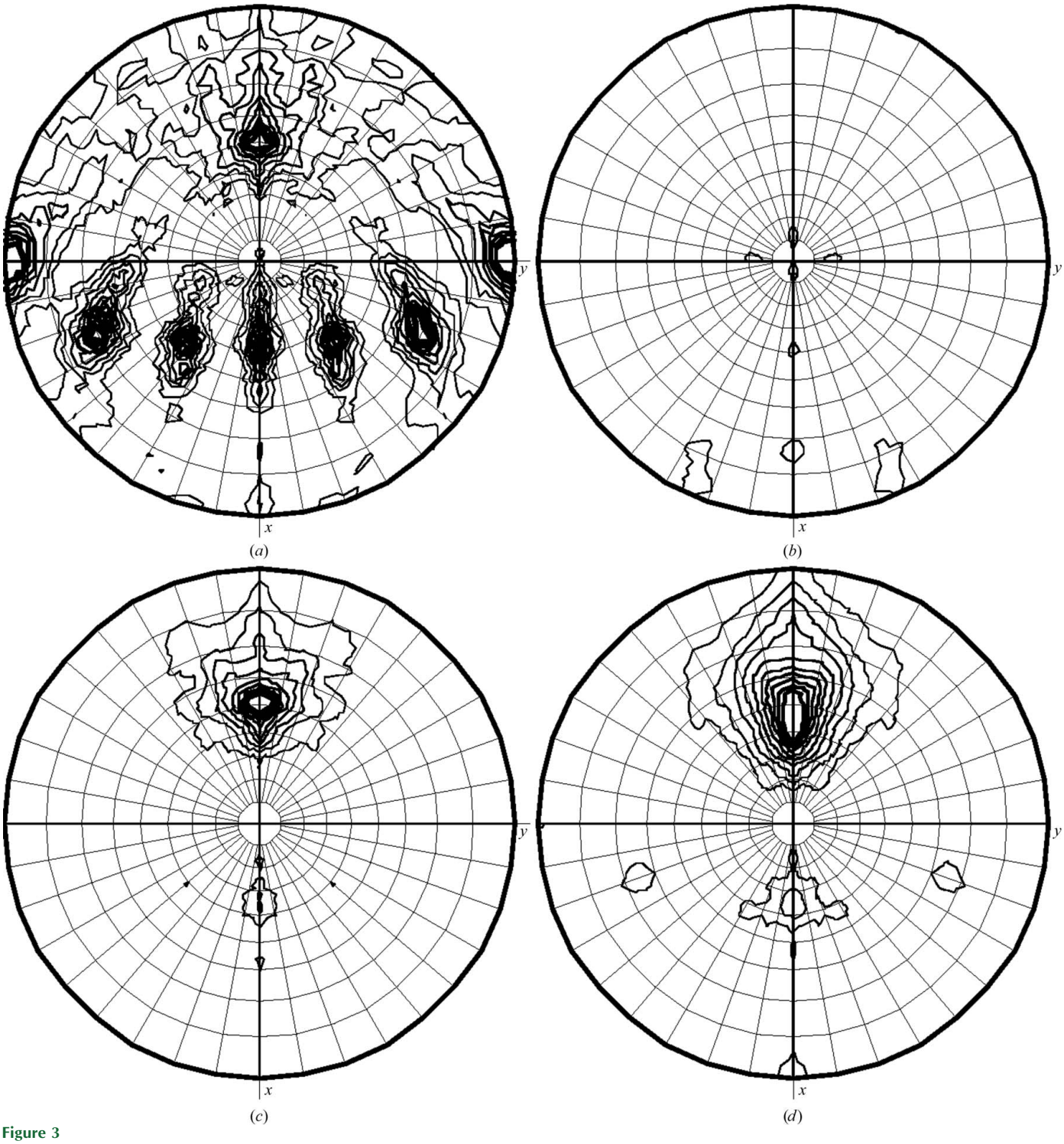

Figure 3
Stereographic projections of various sections of the self-rotation function calculated using data for the SOD-TAT crystal: (*a*) $\kappa = 180^\circ$, (*b*) $\kappa = 90^\circ$, (*c*) $\kappa = 120^\circ$, (*d*) $\kappa = 60^\circ$.

unit-cell parameters a = 181.83, b = 112.58, c = 82.57 Å, $\beta = 111.74^\circ$. Diffraction data were collected and processed (Table 1) with a final $R_{\rm merge}$ value of 11.5% (39.3% for the highest resolution shell). The data completeness, data multiplicity and average $I/\sigma(I)$ value of the collected data set were 95.5%, 20.4 and 14.1, respectively (96.9%, 20.4 and 3.0, respectively, for the highest resolution shell).

Self-rotation function computations using the program *MOLREP* from the *CCP*4 suite (Winn *et al.*, 2011) confirmed the presence of NCS sixfold axes ($\chi = 60^\circ$ section; Fig. 3). Based on consideration of the Matthews coefficient, the most probable number of SOD-TAT molecules in the asymmetric unit is six. In this case the Matthews coefficient is 3.85 Å^3 Da^{-1}, corresponding to a solvent content of 68.03%. Molecular replacement and structure refinement are currently in progress.

We are grateful to the staff of beamline BL17U1 at the Shanghai Synchrotron Radiation Facility for excellent technical assistance

during data collection. This work was supported by grants from the National Natural Science Foundation of China (grant Nos. 30800285 and 31071497) and the Joint Research Project of Fujian Province Educational Committee and Health Department (grant No. WKJ2008-2-47).

References

Josephson, L., Tung, C.-H., Moore, A. & Weissleder, R. (1999). *Bioconjug. Chem.* **10**, 186–191.
Kim, D. W. *et al.* (2005). *Mol. Cells*, **19**, 88–96.
Kwon, H. Y., Eum, W. S., Jang, H. W., Kang, J. H., Ryu, J., Lee, B. R., Jin, L. H., Park, J. & Choi, S. Y. (2000). *FEBS Lett.* **485**, 163–167.
Lewin, M., Carlesso, N., Tung, C.-H., Tang, X.-W., Cory, D., Scadden, D. T. & Weissleder, R. (2000). *Nature Biotechnol.* **18**, 410–414.
Liu, S.-T., Saito, A., Azakami, H. & Kato, A. (2003). *Protein Expr. Purif.* **27**, 304–312.
Otwinowski, Z. & Minor, W. (1997). *Methods Enzymol.* **276**, 307–326.
Pan, J., Peng, S., Zhou, J., He, H., Liu, S. & Rao, P. (2010). *Radiat. Prot.* **30**, 209–213.
Pan, J., Zhou, J., Peng, S., He, H., Liu, S. & Rao, P. (2009). *J. Radiat. Res. Radiat. Process.* **27**, 297–302.
Quinlan, T., Spivack, S. & Mossman, B. T. (1994). *Environ. Health Perspect.* **102**, Suppl. 2, 79–87.
Tsan, M.-F. (1997). *Proc. Soc. Exp. Biol. Med.* **214**, 107–113.
Wadia, J. S. & Dowdy, S. F. (2002). *Curr. Opin. Biotechnol.* **13**, 52–56.
Winn, M. D. *et al.* (2011). *Acta Cryst.* D**67**, 235–242.